JX-ISAS-SUZAKU-MEMO-2008-03
Title: Improvement and Reproducibility of the HXD-PIN Non X-ray Background for the ver 2.0 Processing Data
Category: HXD
Author: T. Mizuno et al.
Date: 2008-05-28

Improvement and Reproducibility of the HXD-PIN Non X-ray Background for the ver 2.0 Processing Data

T. Mizuno, Y. Fukazawa, H. Takahashi,
M. Ushio, S. Yamada,
M. Kokubun, S. Watanabe and the HXD team
e-mail: mizuno@hep01.hepl.hiroshima-u.ac.jp

Last updated on May 28, 2008

1 Introduction

The Si-PIN diodes of the HXD (Hard X-ray Detector) are designed to reduce an instrumental background (non X-ray background; NXB) as much as possible (Takahashi et al. 2007), and achieves an unprecedented low background in the energy range of 15–70 keV (Kokubun et al. 2007). This low background enables us to study spectral shape and time variability of objects accurately around 20–40 keV. A limiting factor for the sensitivity is a reproducibility in the background estimation, together with the statistical error.

Since the beginning of the ver 2.0 pipeline processing, a PIN background model utilizing a PIN Upper Discriminator count rate and its build-up (so-called "bgd_a" model with a `METHOD` keyword of `PINUDLCUNIT`) has been supplied [1]. Since this model is provided as a quick version so that observers can start data analysis of objects with moderate intensity as soon as possible, the reproducibility of the NXB is not optimized (e.g., Mizuno et al. 2007). Apart from this model, the HXD team has been developing another one (so-called "bgd_d" model, `METHOD=LCFIT`) based on the GSO background modeling (Fukazawa et al. 2007). Because this method uses the calibrated GSO data for the background monitor, the model file can be generated only after the release of the GSO gain history file normally at the beginning of each month. Therefore, this PIN background model can be released 1–2 months after the release of the observational data, but is expected to reproduce the NXB better. Here we briefly describe the modeling method and report the reproducibility of the PIN NXB.

2 Modeling Method

In Figure 1, the 15–40 keV PIN NXB count rate obtained during Earth occultation is plotted against the `astetime` over 2 years since the launch. Contrary to the GSO, the count rate of the

[1] http://www.astro.isas.jaxa.jp/suzaku/analysis/hxd/pinnxb/pinnxb_ver2.0

PIN does not increase due to the buildup of radio-activation. Therefore, the PIN background level has been kept to be the lowest since the launch. As indicated by the figure, the NXB count rate was lower than usual while the GSO LD level was changed, and this decrease of the background has already been taken into account in the modeling of "bgd_d". The outline of the modeling method is described in Fukazawa et al. (2007). The latest version (with `METHODV` keyword of "`2.0ver0804`") includes several improvements (and bug-fixes), of which the most important two will be described below.

The first one is the correction of weak dependencies on the Earth elevation angle, cut-off rigidity, satellite altitude and geomagnetic field. Among them, the correction for the Earth elevation angle dependence is the most important, because we assume that Earth occultation data are equivalent to the PIN NXB during observations of celestial objects. Figure 2 left compares count rates between the data and the background model BEFORE the correction of dependencies. Data points at the negative elevation angle correspond to the Earth occultation, and those at the positive elevation angle correspond to observations of dark objects for the PIN. A weak (a few % level) negative correlation between the residual and the elevation angle is seen. The step around 0 degree corresponds to the CXB level. The comparison AFTER the correction is given in the right panel and does not show significant elevation angle dependence.

The second improvement is the dead-time correction. Contrary to the quick-version of the PIN NXB model ("bgd_a" model; `METHOD=PINUDLCUNIT`), the original "bgd_d" model (either for PIN or GSO) does not include the dead-time correction. In order to avoid the possible confusion, we applied the dead-time correction to the "bgd_d" model (`METHOD=LCFIT`) and hereafter supply the dead-time corrected "bgd_d" model (`METHOD=LCFITDT`). Therefore, user can use the PIN background model of "bgd_a" and "bgd_d" in the same way. Note that as of May 2008, GSO background model has not included the dead-time correction yet.

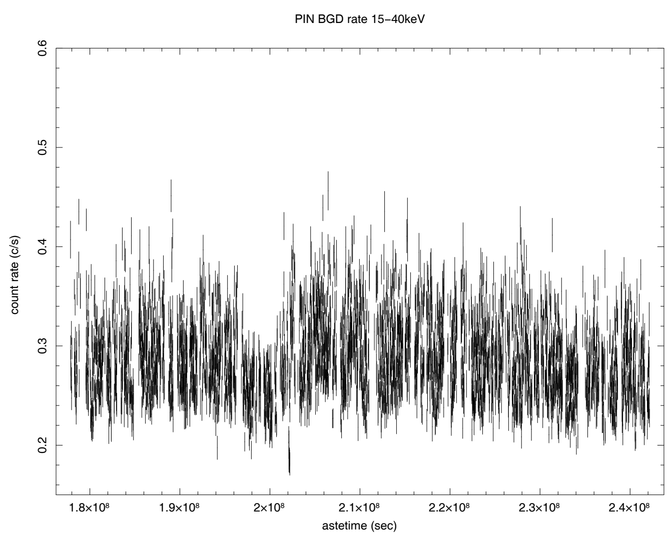

Figure 1: Time history of the PIN NXB count rate in 15–40 keV taken during the Earth occultation. The period of low count rate (`astetime` from $\sim 1.97 \times 10^8$ s to $\sim 2.11 \times 10^8$ s) corresponds to 2006/03/23 – 2006/05/13 while the GSO LD level was changed.

3 Reproducibility in the HXD-PIN NXB

In this section, we examine the reproducibility of the HXD-PIN NXB by utilizing the available Earth occultation data and the sky data with no know strong hard X-ray sources. The event

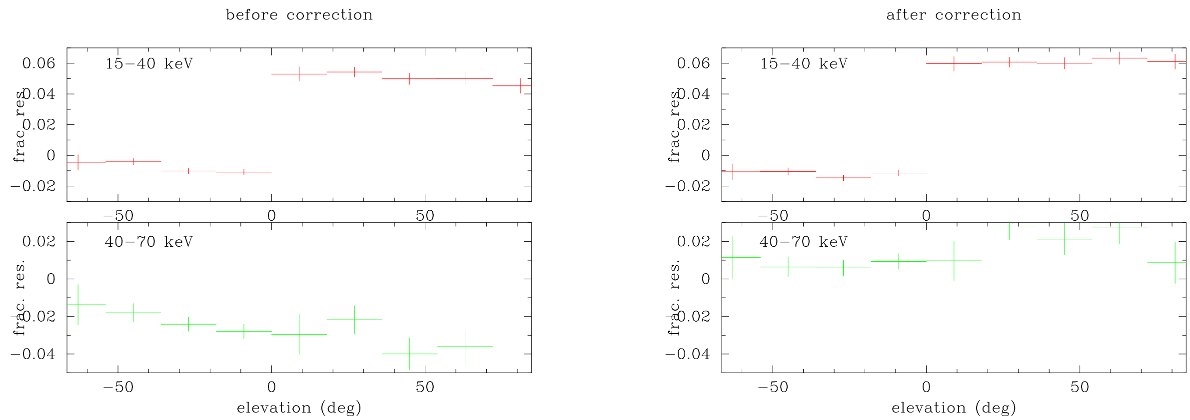

Figure 2: The data - NXB model rate (fractional) against the Earth elevation angle. Left and right panel show the residual before and after the correction of the elevation angle dependence (and dependencies on other parameters such as cut-off rigidity), respectively.

selection criteria are the same as those of cleaned event. To be specific, we applied the following selection criteria: the cut-off rigidity is greater than 6 GV (`COR>6`), the elapsed time after the passage of SAA (South Atlantic Anomaly) is more than 500 s and the time to the next SAA passage is more than 180 s (`T_SAA_HXD>500 && TN_SAA_HXD>180`), high voltages from all eight HV units are in normal value (`HXD_HV_W[0123]_CAL>700 && HXD_HV_T[0123]_CAL>700`) and the satellite is in pointing mode and the satellite position is stabilized (`AOCU_HK_CNT3_NML_P==1 && ANG_DIST<1.5`). Elevation angle from the Earth rim is more than 5° (`ELV>5`) or less than -5° (`ELV<-5`) for sky and Earth observation, respectively. We also use `hxdgtigen` to discard the time interval when the telemetry was saturated.

3.1 Data/model spectra of integrated Earth occultation data

Figure 3 compares energy spectra between the data and the NXB model during the Earth occultation of all available data as of May 2008 (7.9 Ms exposure in total). We see a very good agreement of the model with the data, and can conclude that they agree within $\sim 1\%$ in 15–70 keV WHEN Earth occultation data are averaged. Small but systematic deviation is seen around 15 keV.

3.2 Comparison with each Earth data

In order to study the background reproducibility quantitatively, we split each observation into small pieces with 10 ks exposure to Earth and compared the NXB count rate between the data and the model in 15–40 keV and 40–70 keV range as shown in Figure 4. We see the model reproduces the data in 15–40 keV within $\pm 7\%$. More quantitatively, the average of the residual is -0.62% and the standard deviation is 2.31%, whereas the statistical error (1σ) is 1.93%, resulting in the systematic uncertainty of about 1.3%. This systematic uncertainty is less than half of that by the "bgd_a" model (Mizuno et al. 2007) and thus the statistical error now dominates the residual. We understand the negative mean of the residual (-0.62%) is due to the "dip" around 15 keV in Figure 3 right. In 40–70 keV the statistical error dominates the residual: the average of the residual is 0.81% and the standard deviation and the statistical error is 4.92% and 4.25%, respectively. We note that the standard deviation of residuals in high energy band is comparable to that of the "bgd_a" model (`METHOD=PINUDLCUNIT`). The time history of residuals is given in

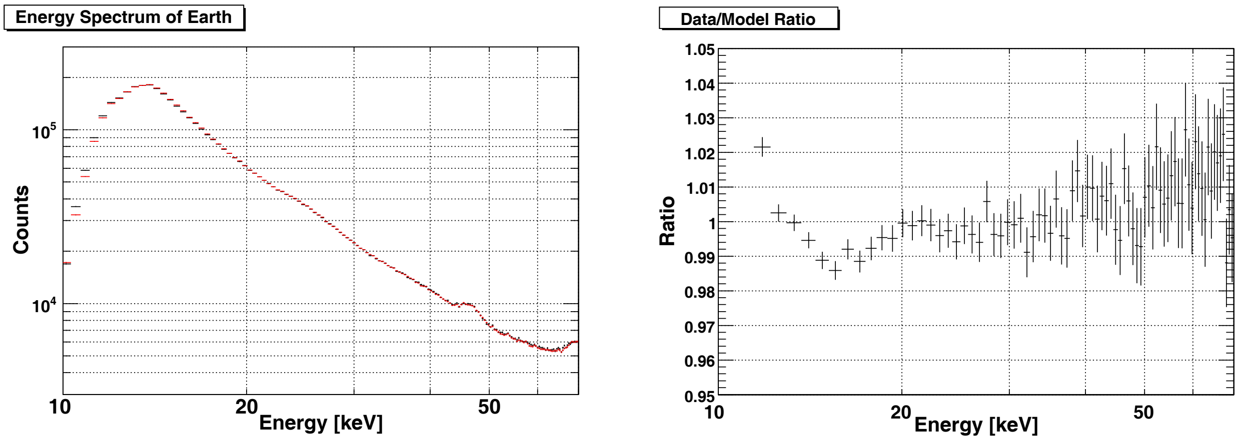

Figure 3: Comparison of spectra between the data and the background model prediction of all the available Earth occultation data as of May 2008 (7.9 Ms exposure). (Left) Unbinned spectra of the data and the model shown by black and red histograms, respectively. (Right) The data to model ratio.

Figure 5 and no significant fluctuation is seen in both energy bands.

We did the same comparison but with a longer integration time as summarized in Figure 6, and observe the NXB reproducibility is improved. The average, the standard deviation and the statistical error of residuals in 15–40 keV is -0.58%, 1.00% and 0.97%, respectively. This results in the systematic uncertainty of about 0.3%. For 40–70 keV, the average of the residual is 0.70% and the standard deviation and the statistical error is 2.89% and 2.14%, respectively, resulting in the systematic uncertainty of about 1.9% which is comparable to the statistical error.

3.3 Comparison with data of dark objects

The reproducibility evaluated in the previous subsection is not necessarily applicable to the observation of celestial objects, due to, e.g., the fluctuation of the cosmic X-ray background (CXB) and different environments of the satellite that could affect the PIN NXB (although we make it minimum with our best efforts as described in § 2). We therefore assess the NXB reproducibility by utilizing the sky observation with no apparent strong hard X-ray objects below.

comparison with each sky data

We first utilized the XIS FI data and selected observations with no strong X-ray emission above 7 keV (less than 20% above the XIS-FI NXB in entire XIS field-of-view) and compared the HXD-PIN data and the NXB model count rate (10 ks exposure) in 15–40 keV, as shown in Figure 7. Here we plotted the residual histogram in unit of count rate, not in the ratio to the NXB model, since we expect a constant excess above 0 due to the CXB emission. The standard deviation (including statistical error) of the residual is 0.0104 c/s, or about 3.5% of the mean NXB count rate, which is much larger than that obtained from the Earth occultation data ($\sim$ 2.3%; see § 3.2). Is this because the systematic uncertainty increases when observing the sky? Or is this due to the reason other than the NXB model accuracy, such as the source contamination or fluctuation of the CXB?

Figure 8 shows the same comparison of sky data and the NXB model for E0102-72 observations in which the same region of the sky is observed regularly for the XIS calibration purpose. Some observations do not satisfy the selection criteria using XIS due to sources or diffuse emission in

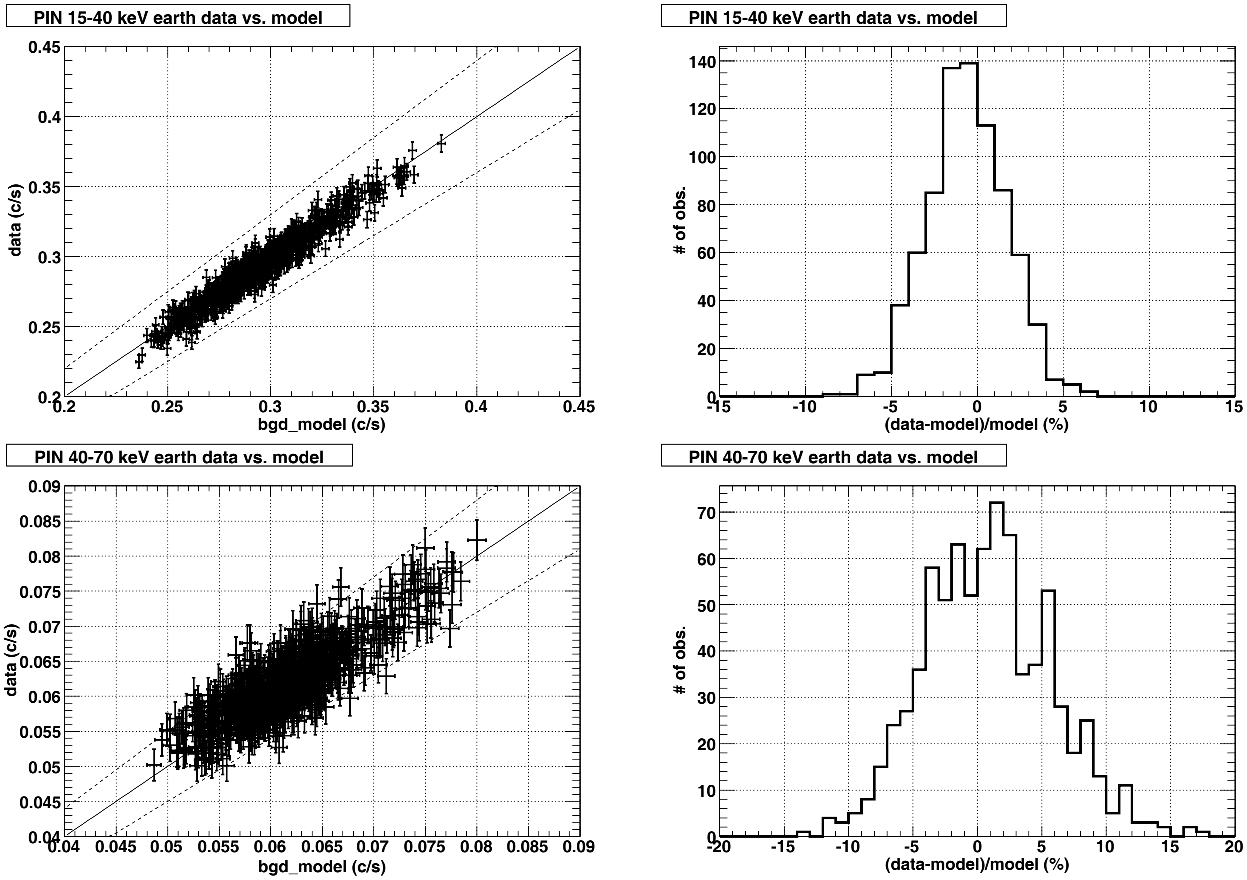

Figure 4: (Top left) A comparison of the NXB count rate in 15–40 keV between the Earth occultation data and the model prediction. (Top right) The residuals in a histogram. (Bottom) The same plots as those in top panels, but in 40–70 keV instead of 15–40 keV.

XIS field-of-view, but we used all E0102 observations in order to compare sky data and the NXB model in as many data as possible. We also plotted the data and the NXB model of Cygnus LOOP multi-pointing observations in red, since regions nearby (within 1.5 degree in radius) are observed. We see a clear difference of the residual between two sets of observations and that the width of the residual for E0102 data is much narrower than that of Figure 7. A 90% confidence region of the residual (including statistical error) obtained from E0102 observations is $\pm \sim 0.015$ c s^{-1}, or $\pm \sim 5\%$ of the mean NXB rate. This is somewhat larger, but comparable to, the residual distribution obtained from Earth occultation data in § 3.2 (standard deviation of 2.31% corresponds to $\pm \sim 3.8\%$ in 90% confidence). As described above, the E0102 data might suffer contamination from sources within field-of-view, and thus this confidence region should be regarded as a conservative estimate. The difference of residuals between two data sets by 0.01–0.015 c s^{-1} could be, again, due to a weak hard X-ray emission inside the PIN field-of-view of E0102 observations.

IF we assume the Cygnus LOOP region is free from any weak hard X-ray emission, we can regard the averaged spectrum as a sum of the CXB plus the NXB. The NXB-model-subtracted spectrum is compared with the spectrum of the CXB model by Boldt (1987) [2] in Figure 9. We see a very good agreement between the subtracted spectrum (green crosses) and the CXB model

[2]Spectral model is $9.412 \times 10^{-3} \times (E/\mathrm{keV})^{-1.29} \times \exp(-E/40\ \mathrm{keV})$ [photons s^{-1} cm^{-2} keV^{-1} FOV^{-1}]. For more detail, see http://heasarc.gsfc.nasa.gov/docs/suzaku/analysis/abc/node10.html.

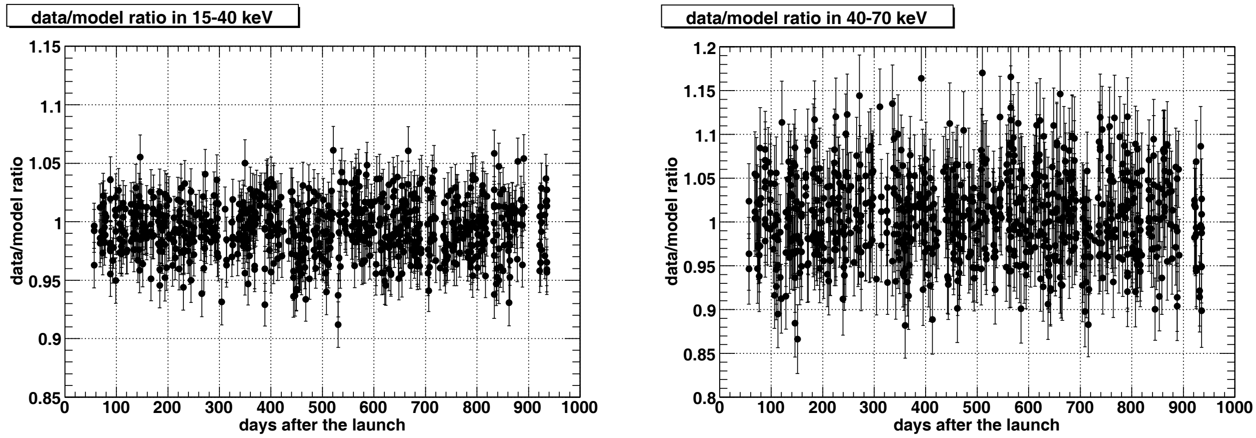

Figure 5: Data to model ratios of the NXB count rate of Earth occultation data, in 15–40 keV(left) and 40–70 keV(right) plotted against the day since 2005 July 10 (the day of Suzaku launch).

(blue ones). We note that the fluctuation of the residual is large (see red histograms in Figure 8 right), and a more detailed examination is necessary to give a firm conclusion on the absolute CXB level above 15 keV.

reproducibility in a single observation

In order to check the NXB reproducibility in a single observation, we also compared the spectrum and the light curve of eight objects whose signal is expected to be negligible for the HXD-PIN. The comparison of spectra are summarized in Figure 10. The background-subtracted spectrum and the CXB model by Boldt 1987 is given in blue and green histograms, respectively. No systematic difference is seen between them up to 60 keV. We also compared the data and the NXB model light curves as summarized in Figure 11 in 15–40 keV band with a time bin of 10 ks. Residuals are consistent with the CXB level in $\pm \sim 0.02$ c s^{-1}, or $\sim 7\%$ of the total NXB count rate.

4 Some cautions

You must take caution to data during which the HXD observation mode was changed. Such operations were performed during the Earth occultation for calibration or during on-source observations when the PIN was noisy. See `http://www.astro.isas.jaxa.jp/suzaku/log/hxd/` to check whether your data includes such operations or not. Since the PIN background model utilizes the count rate of the PIN Upper Discriminator, the background model is affected for these observations. Especially, the data during May 24 to 29 in 2006 suffers PIN noise significantly, and you must select PINs on WPU board 0, 1 or 2 for both the data and the background model. Since this period is short and thus the database of the Earth occultation for constructing the background model is not large enough, the reproducibility is somewhat worse, probably $\sim 10\%$.

Reference

- Takahashi, T. et al. 2007, PASJ 59, S35
- Kokubun, M. et al. 2007, PASJ 59, S53

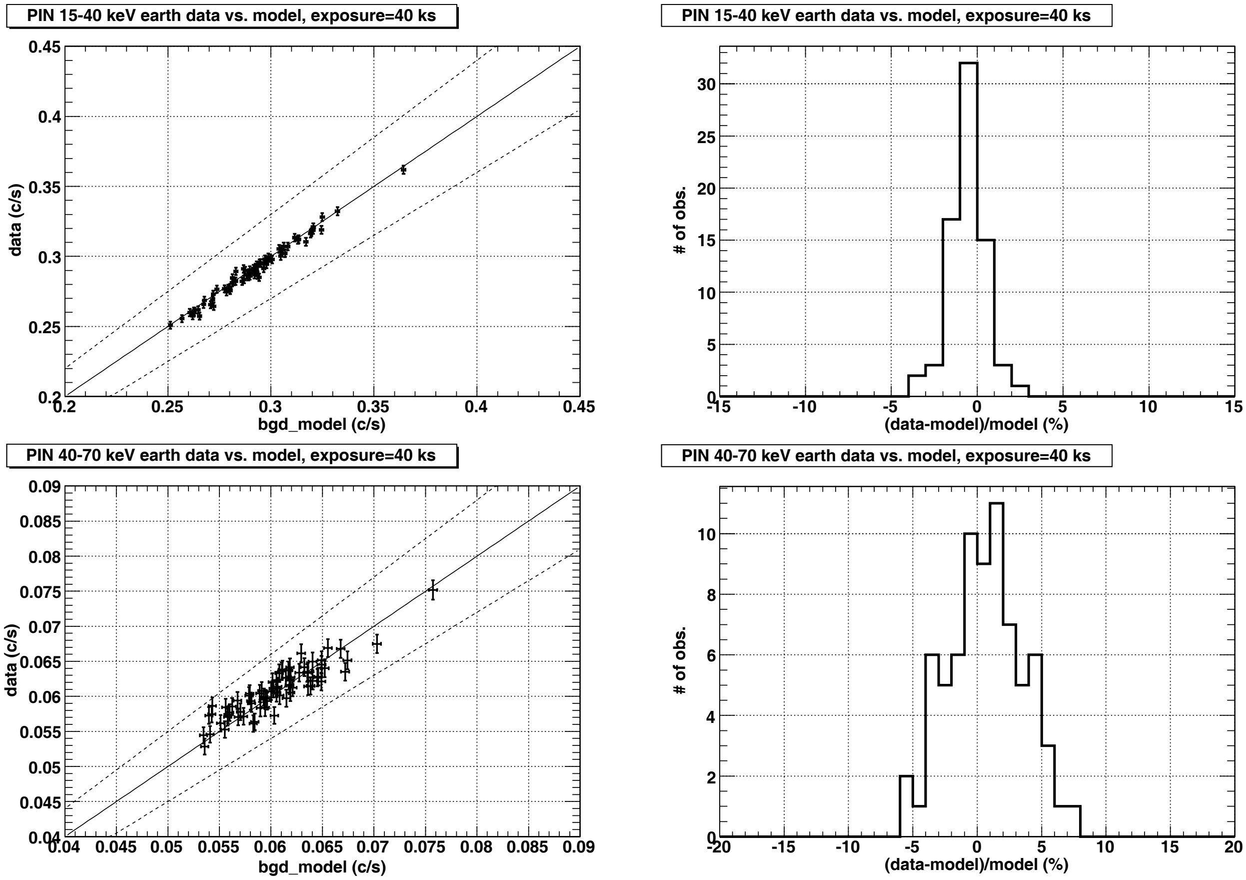

Figure 6: The same plots at those of Figure 4, but the integration time is 40 ks instead of 10 ks.

- Mizuno, T. et al. 2007, SUZAKUMEMO-2007-09
- Fukazawa, Y. et al. 2007, SUZAKUMEMO-2007-02
- Boldt, E. 1987, IAU circ. 124, 611

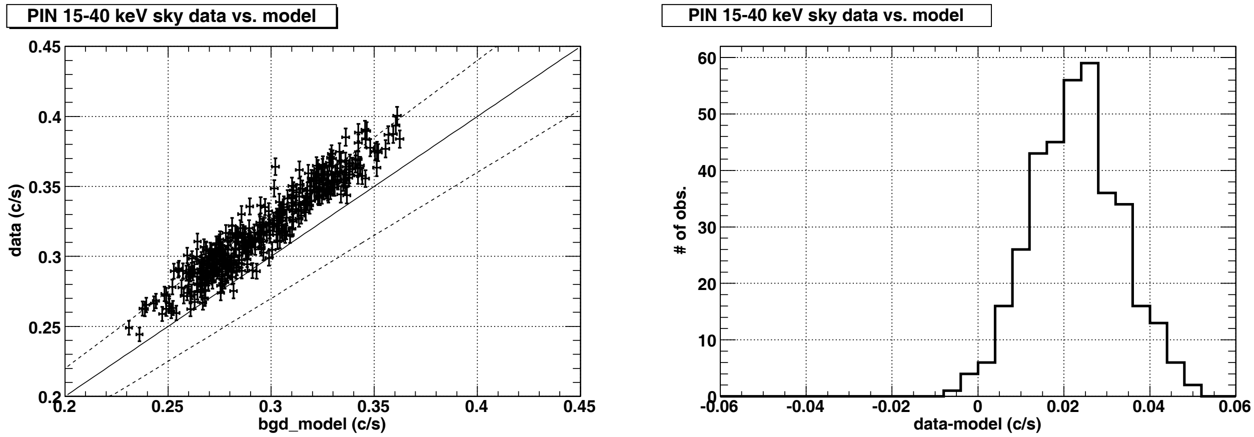

Figure 7: Comparisons between the data and the NXB model count rate of sky observations with 10 ks integration time. Observations with no apparent hard X-ray objects in XIS FOV are selected (see text for details of the data selection).

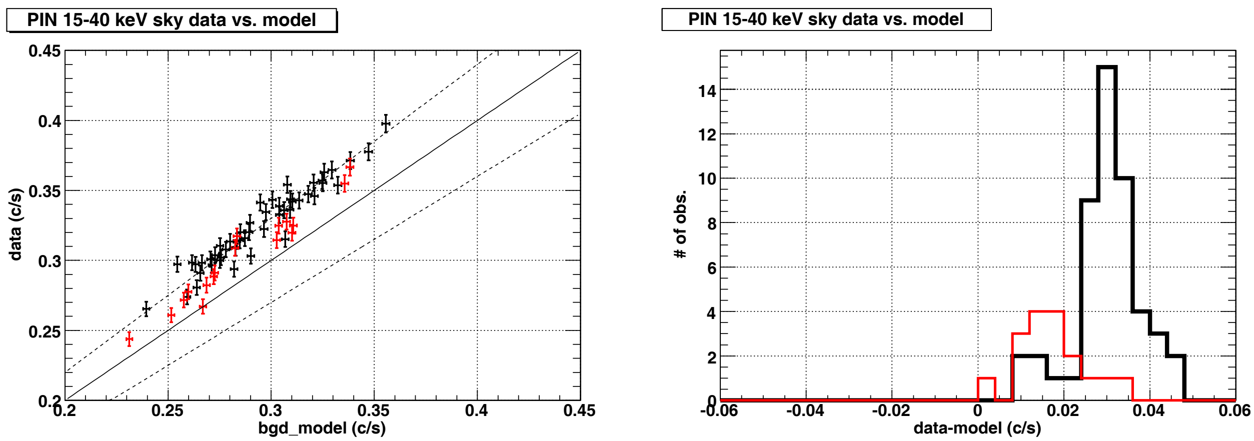

Figure 8: The same as Figure 7, but observations of E0102 (black) and Cygnus LOOP multi-pointing (red) are used.

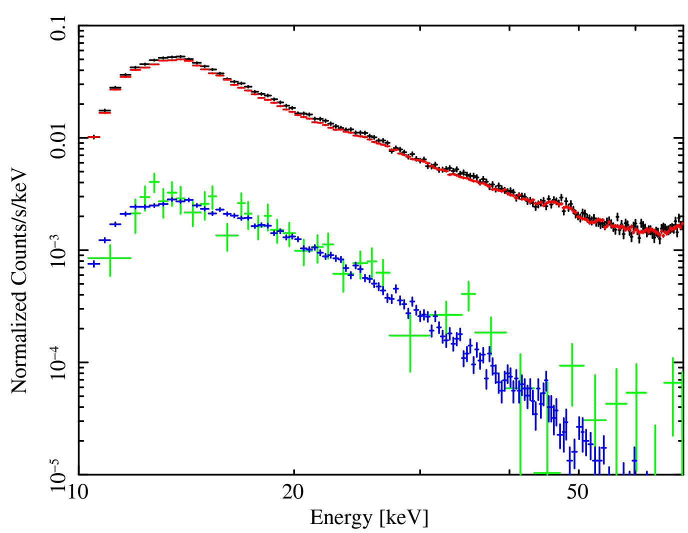

Figure 9: Averaged spectra of sky observations (black) and the NXB model (red) of Cygnus LOOP multi-pointing observations, together with the subtracted spectrum (green) and the CXB model (blue) by Boldt (1987).

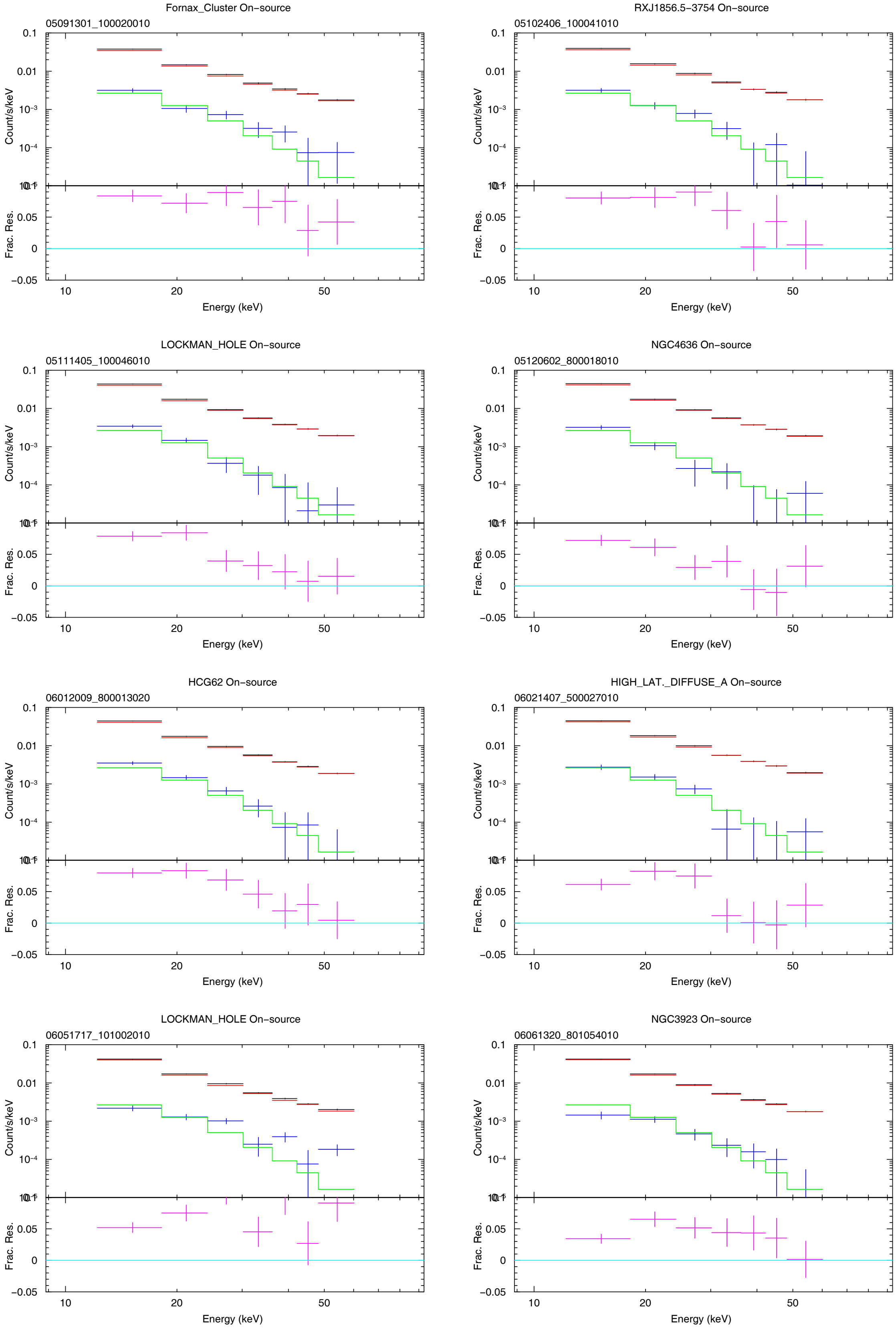

Figure 10: Comparison of spectra between the data (black) and the NXB model (red) for observations of objects with no known strong hard X-rays. Fractional residuals are given by purple crosses in the bottom panel of each figure. The blue and green histograms in the top panel indicate the residual spectrum and the typical CXB spectrum (model by Boldt 1987), respectively.

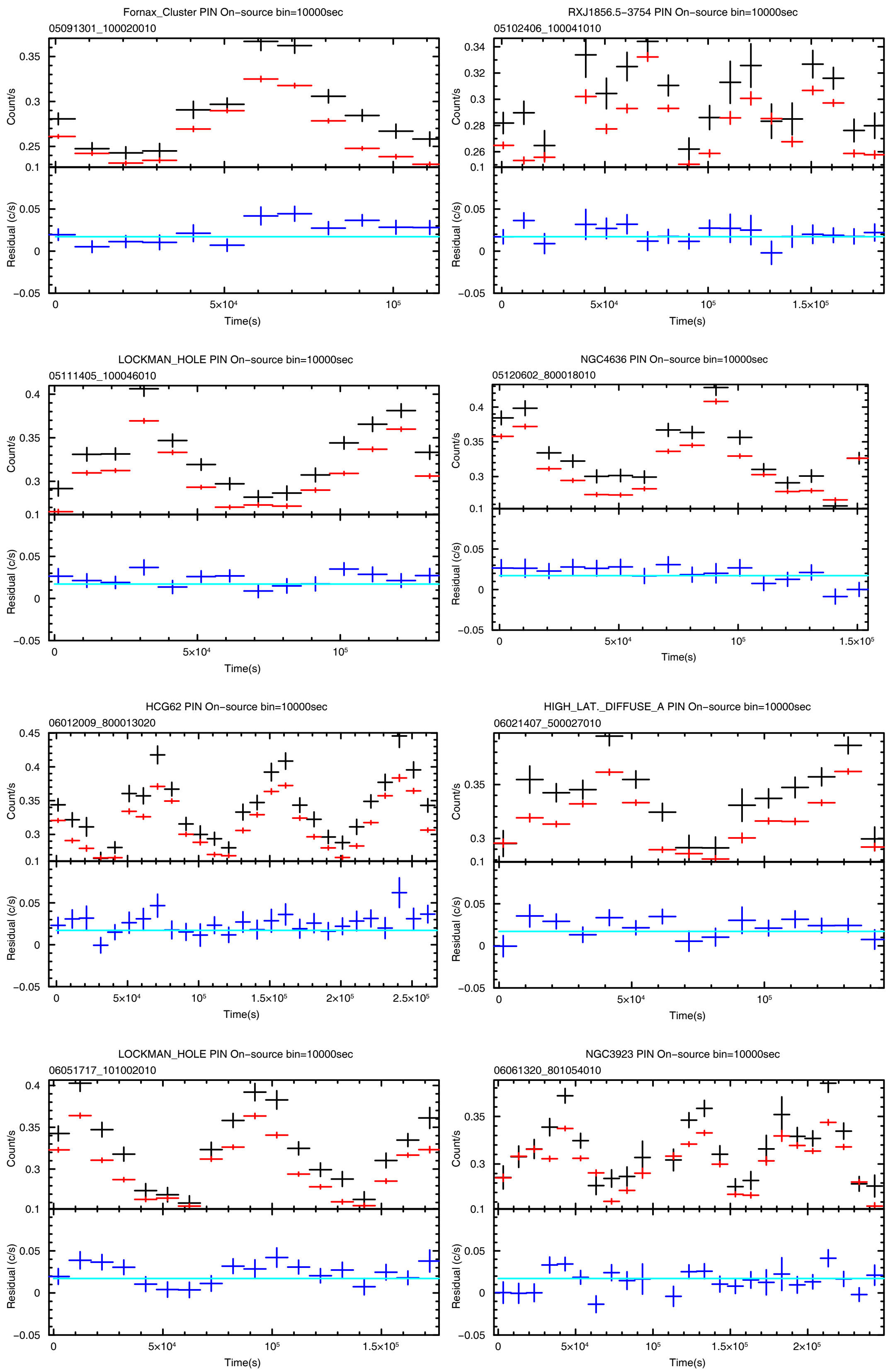

Figure 11: The same as Figure 10 but for 15–40 keV light curves instead of spectra. In each panel, the upper figure shows the light curve and the lower figure shows the residuals. A time bin width is 10 ks. The horizontal line in the bottom panels in each figure indicates the CXB level.